*Proc. Nat. Acad. Sci. USA*
Vol. 73, No. 2, pp. 432–436, February 1976
Biochemistry

# Molecular orbital studies of enzyme activity: Catalytic mechanism of serine proteinases*

**(partial retention of diatomic differential overlap/trypsin)**

STEVE SCHEINER AND WILLIAM N. LIPSCOMB†

Gibbs Chemical Laboratory, Harvard University, Cambridge, Massachusetts 02138

*Contributed by William N. Lipscomb, December 1, 1975*

**ABSTRACT** **The catalytic activity of the serine proteinases is studied using molecular orbital methods on a model of the enzyme–substrate complex. A mechanism is employed in which Ser-195, upon donating a proton to the His-57–Asp-102 dyad, attacks the substrate to form the tetrahedral intermediate. As His-57 then donates a proton to the leaving group, the intermediate decomposes to the acyl enzyme. An analogous process takes place during deacylation, as a water molecule takes the place of Ser-195 as the nucleophile. The motility of the histidine is found to be an important factor in both steps. An attempt is made to include the effects of those atoms not explicitly included in the calculations and to compare the reaction rate of the proposed mechanism with that of the uncatalyzed hydrolysis. This mechanism is found to be in good agreement with structural and kinetic data.**

It has been determined that the chymotrypsin-catalyzed hydrolysis of substrates proceeds through an acyl enzyme intermediate (1). The formation of a tetrahedral intermediate in the acylation step of trypsin was investigated in Paper I (2), in which molecular orbital methods were used to study the charge relay system (3) and the attack of the serine residue on the scissile peptide linkage of the substrate. We report here a continuation of this work which includes both the acylation and deacylation steps in their entireties. The principal method used is partial retention of diatomic differential overlap (PRDDO), which closely reproduces minimum basis set (MBS) *ab initio* results (4). Also included are terms which correct the errors introduced by use of an MBS.

## RESULTS

The active site residues of trypsin were modeled as follows: Ser-195‡ by methanol, His-57 by imidazole, the Asp-102 anion by formate, and the scissile peptide linkage of the substrate by formamide. As described in Paper I, these molecules were then superimposed onto Huber's x-ray structure of the complex of bovine trypsin with bovine pancreatic trypsin inhibitor (5). In this structure, the scissile peptide link is distorted towards a tetrahedral carbon. However, when methanol is included at its x-ray position, a geometry optimization of formamide yielded a very nearly planar carbonyl group (see Fig. 1A). When the orientation of imidazole was optimized with respect to rotations about the $C^{\alpha}$-$C^{\beta}$ and $C^{\gamma}$-$C^{\beta}$ bonds of His-57, we found a nearly bifurcated hydrogen bond between $N^{\delta 1}$ and formate. The preferred orientation of methanol with respect to a rotation about its $C_s$-$H_{s1}$ bond axis (corresponding to the $C^{\beta}$-$C^{\alpha}$ axis of Ser-195) is that of the x-ray structure. The configuration thus obtained, analogous to the bound enzyme–substrate Michaelis complex, E·S, is shown as A in Fig. 1.

We followed the formation of the tetrasubstituted intermediate (TI) as the composite of two separate processes. The first of these involved proton transfers from methanol to $N^{\epsilon 2}$ of imidazole and, simultaneously, from $N^{\delta 1}$ of imidazole to $O_{a2}$ of formate. The remaining geometry changes involved in the formation of the TI comprise the second. The most significant motions included here were (*1*) the rotation of methoxide around the $C_s$-$H_{s1}$ bond axis by 30° to attack $C_f$, (*2*) a motion of $C_f$ up out of the carbonyl plane towards the approaching $O_s$ to form the tetrahedral adduct, and (*3*) the rotation of imidazole down towards $O_s$, maintaining the $O_s$-$N^{\epsilon 2}$ hydrogen bond. A projection of the potential energy surface into the subspace defined by these two processes indicated that the methoxide attack does not begin until the proton transfers are about 80% complete. The transition state (TS) is encountered at half proton transfer, from which the reaction proceeds energetically downhill to the intermediate.

In order to obtain a quantitative estimate of the MBS errors (MBSE) which are a result of the inability of a MBS to deal adequately with the high electron density present on certain anions, the proton transfer

$$AH + NH_3 \longrightarrow A^{\delta-}\!\!-\!\!H\!\!-\!\!^{\delta+}NH_3 \longrightarrow A^- + NH_4^+ \quad [1]$$

was monitored by both the PRDDO-MBS and 4-31G (6) methods. We define $E(x)$ as the energy required to lengthen the A-H bond by some amount $x$, and we define MBSE($x$) as $E_{\mathrm{PRDDO}}(x) - E_{4\text{-}31G}(x)$. For AH = $CH_3OH$, HCOOH, or $H_2O$ we found a nearly linear relationship between $MBSE_A$ and the PRDDO Mulliken group charge on A, $q_A$: $MBSE_A = c_A|q_A - q_A^{\circ}|$. Values of $c$ and $q^{\circ}$ are shown in Table 1.

When $CH_3O^-$ adds to $HCONH_2$ to form the "tetrahedral" adduct, we find that the MBSE of the adduct is 50 kcal/mol less than that of the reactants (7). As $HCONH_2$ is an electronically neutral species and, as such, would not be expected to have a large MBSE, we assume that

$$MBSE_{CH_3OCHONH_2^-} = MBSE_{CH_3O^-} - 50 \text{ kcal/mol} \quad [2]$$

and scale $c$ for the adduct accordingly, i.e.,

$$c_{CH_3OCHONH_2^-} = c_{CH_3O^-} \times (MBSE_{CH_3OCHONH_2^-}/MBSE_{CH_3O^-}) \quad [3]$$

The negative of the charge of a third proton placed on N to form $CH_3OCHONH_3$ was taken as $q^{\circ}$ for this species (Table 1). Since the proton affinity of the species $CH_3OCHO(OH)^-$ is calculated by PRDDO to be nearly identical to that of

Abbreviations: PRDDO, partial retention of diatomic differential overlap; MBS(E), minimum basis set (error); TI, tetrasubstituted intermediate; TS, transition state.

* Presented by S.S. at the Third East Coast Protein Crystallography Workshop in Lenox, Mass., October 27, 1975. This is Paper III of a series.

† Author to whom reprint requests should be sent.

‡ We use the chymotrypsin numbering system to identify the amino-acid residues.

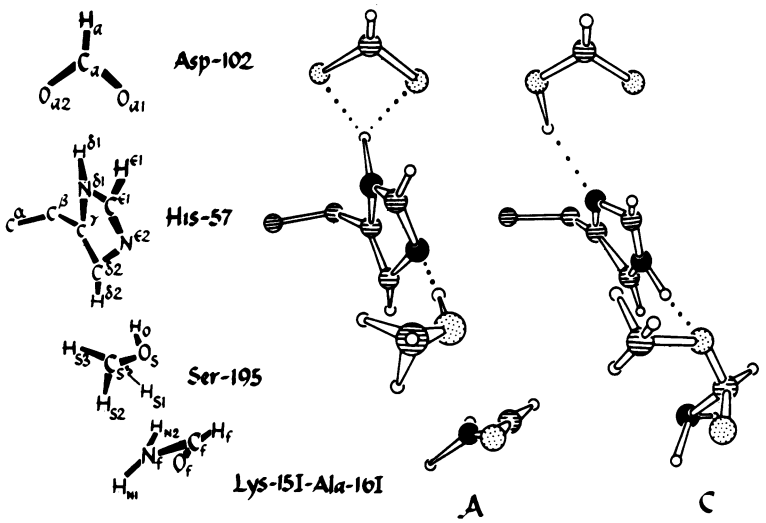


FIG. 1. Atomic positions for configurations A and C. Dotted lines represent hydrogen bonds. Note that $C^{\alpha}$ and $C^{\beta}$ of His-57 are shown here as reference points for orientation changes in imidazole even though they are not explicitly included in the calculations.

$CH_3OCHO(NH_2)^-$ the same values of $c$ and $q^\circ$ were used for both.

As a refinement of the work presented in Paper I, a more extensive optimization was performed on the geometry of the tetrahedral adduct obtained in that study. In this, as in all optimizations below, $C_f$ was held stationary and $r(C_f—O_s)$ was allowed to vary but the coordinates of the $CH_3O$ group were otherwise fixed. $r(C_f—H_f)$ was held constant, as was the $C_f—N_f$ bond direction. The resulting bond lengths within the adduct are presented in Table 2. Application of the MBSE corrections to the TI thus obtained (C in Fig. 1), the TS (B) and the starting point (A) yields the energy profile shown in Fig. 2. The explicit inclusion of MBSE corrections here is responsible for the difference between this profile and Fig. 3 of Paper I.

The breakdown of the TI is hypothesized to involve a proton transfer from $N^{\epsilon 2}$ of His-57 to the leaving group nitrogen (8). In order to avoid the production of the highly unstable imidazole anion, an analogous process in our model system must also include the transfer of $H^{\delta 1}$ back to $N^{\delta 1}$ from $O_{a2}$ (see Fig. 1). Regardless of the position of imidazole, at least one of the protons will have to be transferred along a very weak or nonexistent hydrogen bond. This is a consequence of the large distance between $O_{a2}$ and $N_f$ (9.0 Å). A simultaneous transfer of the two protons resulted in a calculated energy barrier of about 100 kcal/mol. Thus the two transfers must occur in a step-wise fashion. The imidazole first moves up toward HCOOH by 0.5 Å (D in Fig. 2 and Table 3). $H^{\delta 1}$ is then transferred (E) from $O_{a2}$ to $N^{\delta 1}$. (Suitable CO bond length alterations in formate accompany all such transfers.) As the positively charged imidazole then swings down towards $N_f$, it passes through an energetically favorable position, at which point there is a strong hydrogen bond between $N^{\epsilon 2}$ and $O_s$. This bond, along with the hydrogen bond between $N^{\delta 1}$ and $HCOO^-$, must be broken when imidazolium rotates down to a position suitable for a proton transfer to $N_f$. In this conformation (F in Fig. 3), a nearly linear hydrogen bond exists between $N^{\epsilon 2}$ and $N_f$; $r(N^{\epsilon 2}—N_f)$ = 2.9 Å. As the proton was transferred to $N_f$, the geometry of the adduct was optimized. The TS (G) for the breakdown of the TI was encountered at half proton transfer where $r(C_f—N_f)$ = 1.75 Å. As the transfer was completed, $NH_3$ was pulled off to $\infty$, leaving behind the planar ester linkage (H). The proton transfer now complete, the imidazole position was once again optimized to yield the acyl enzyme plus $NH_3$(I). The formation of a nearly bifurcated hydrogen bond to formate is primarily responsible for the final ring position in the acyl enzyme (Table 3).

In order to study the analogous hydrolysis of an ester, HCOOH was substituted for $HCONH_2$ as the substrate. We assumed that the model ester substrate will undergo geometry changes during acylation which are quite similar to those of the amide. In all of the configurations involving the ester substrate (see Fig. 2), the $O_eH_e$ group was substituted in the substrate such that the $C_f—O_e$ bond direction coincided with the $C_f—N_f$ direction of the amide and $r(O_e—H_e)$ = 0.97 Å. The $C_f—O_e$ bond length was optimized, as was the angular position of $H_e$. In the initial configuration (A′) as well as the TI (C′), $H_e$ adopted a position *cis* to $O_f$.

The deacylation of the acyl enzyme is hypothesized to proceed analogously to acylation with a water molecule taking the place of Ser-195 as the nucleophile (1). It was, there-

Table 1. Parameters for calculations of MBSE

| Species (A—H) | $c_A$ (kcal/mol) | $q_A^\circ$ |
|---|---|---|
| $CH_3O$—H | 122 | —0.32 |
| HCOO—H | 122 | —0.29 |
| HO—H | 159 | —0.28 |
| $CH_3OCHO(NH_2)$—H<br>$CH_3OCHO(OH)$—H | 68 | —0.36 |

Table 2. Bond lengths (Å) in substrate during hydrolysis

| | Configuration | $C_f—O_s$ | $C_f—O_f$ | $C_f—N_f$* |
|---|---|---|---|---|
| Acylation | | | | |
| A | $E{\cdot}S$ | 2.82 | 1.24 | 1.41(1.38) |
| C | TI | 1.48 | 1.32 | 1.50(1.47) |
| I | Ac—$E + P_1$ | 1.38 | 1.23 | $\infty$ |
| | | | | $C_f—O_w$ |
| Deacylation | | | | |
| J | Ac—$E{\cdot}H_2O$ | 1.38 | 1.23 | 2.56 |
| P | TI | 1.50 | 1.32 | 1.50 |
| R | $E + P_2$ | $\infty$ | 1.24 | 1.38 |

* Values in parentheses refer to $C_f$-$O_e$ bond lengths.

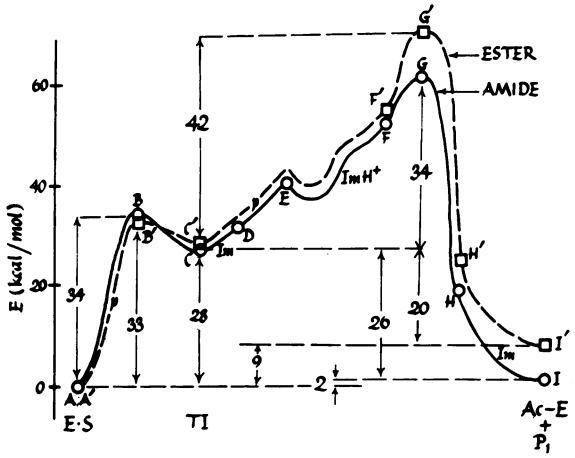


FIG. 2. Energy profile of acylation of the model enzyme. Ac-E refers to the acyl enzyme and $P_1$ to either $NH_3$ or $H_2O$. The symbols along the energy curves indicate the following: p, proton transfer; Im and $ImH^+$, rotation of the neutral and positively charged imidazole, respectively. MBSE corrections have been included for all points shown. The uncorrected PRDDO curve shows (*a*) a barrier of only 7 kcal/mol between points A and C (which is more stable than A), (*b*) no barrier between F and H, and (*c*) E more unstable than D by 60 kcal/mol.

fore, necessary to add a water molecule to our model of the acyl enzyme in a position suitable for subsequent attack on the carbonyl carbon of the ester linkage. It must also be placed so that a proton transfer to $N^{\epsilon 2}$ of imidazole is facilitated. To test the feasibility of a simultaneous transfer of two protons as in the acylation step, a water molecule was added with imidazole in the same position as in configuration D above; i.e., close to formate. Steric interactions prevented the oxygen atom of the water molecule, $O_w$, from being situated any closer than 3.0 Å to either $C_f$ or $N^{\epsilon 2}$, or from lying any nearer than 2.6 Å to the central axis of the ester. (This axis passes through $C_f$ and is orthogonal to the plane of the ester.) In this configuration a simultaneous transfer of one proton from $O_w$ to $N^{\epsilon 2}$ and another from $N^{\delta 1}$ to $O_{a2}$ resulted in a calculated energy barrier of >80 kcal/mol.

With imidazole in approximately the same position from which it donated a proton to the leaving group in the previous step, the water molecule can fit in quite close to $N^{\epsilon 2}$, $C_f$,

Table 3. Imidazole in various configurations

| | Interatomic distances (Å) | | | |
|---|---|---|---|---|
| (α,γ)* | $N^{\delta 1}$—$O_{a_1}$ | $N^{\delta 1}$—$O_{a_2}$ | $N^{\epsilon 2}$—$O_s$ | |
| Acylation | | | | $N^{\epsilon 2}$—$N_f$ |
| A (5°,17°) | 2.58 | 2.81 | 2.66 | 4.40 |
| C (−5°,26°) | 3.03 | 3.15 | 2.79 | 3.73 |
| D (10°,29°) | 2.57 | 2.59 | 3.20 | 4.52 |
| F (−30°,−9°) | 3.74 | 4.24 | 3.11 | 2.93 |
| I (5°,26°) | 2.67 | 2.77 | 3.09 | ∞ |
| Deacylation | | | | $N^{\epsilon 2}$—$O_w$ |
| J (−30°,−4°) | 3.74 | 4.20 | 3.13 | 2.46 |
| M (−5°,15°) | 2.90 | 3.18 | 2.56 | 3.45 |
| N (10°,29°) | 2.57 | 2.59 | 3.04 | 4.29 |
| P (−5°,25°) | 3.02 | 3.15 | 2.57 | 3.47 |
| R (5°,17°) | 2.58 | 2.81 | 2.66 | ∞ |

* Rotations of imidazole from the x-ray structure are designated (α,γ), where α(γ) is the rotation about the $C^{\alpha}$-$C^{\beta}$($C^{\gamma}$-$C^{\beta}$) bond axis of His-57. Positive rotations are counter clockwise ring movements viewed along $C^{\alpha}$ or $C^{\gamma}$ to $C^{\beta}$.

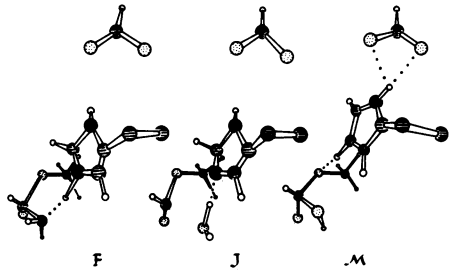


FIG. 3. Atomic positions of three configurations. Of the two protons of the water molecule in J, $H_{w1}$ is hydrogen bonded to imidazole; the other is $H_{w2}$.

and the central axis with a minimum of steric repulsion. The water molecule [r(OH) = 0.97 Å, ∢HOH = 109.4°] was added in the plane defined by the central axis of the ester and $N^{\epsilon 2}$ such that $r(O_w - N^{\epsilon 2})$ = 2.46 Å and $r(O_w - C_f)$ = 2.56 Å. $O_w$ is less than 0.2 Å from the central axis. The most stable orientation is that having a linear hydrogen bond; i.e. $\sphericalangle O_w—H_{w1}—N^{\epsilon 2}$ = 180°. In this configuration (J in Fig. 3) both imidazole and water are "locked" in position; imidazole is at the bottom of a potential well with respect to its two allowed rotations, and water with respect to translations toward either $C_f$ or $N^{\epsilon 2}$. The large distance between imidazole and formate (see Table 3) precludes a proton transfer between these two residues in this configuration. The transfer of a proton from the water will thus result in the production of an imidazolium cation.

The potential energy surface for the formation of the tetrahedral adduct in deacylation was assumed to be qualitatively similar to that of the acylation step.§ As proton $H_{w1}$ was transferred from $O_w$ to $N^{\epsilon 2}$, the energy of the system increased. After about 85% of the full transfer (K) the attack by the hydroxide on the ester was found by the PRDDO method to be energetically favorable. The optimized tetrahedral adduct was then formed¶ as the proton transfer was completed to yield configuration L. During this process (K → L) the energy of the system decreases. The point at which the attack begins (K) is thus the TS for this reaction step. The nucleophilic attack included a translation of hydroxide of 0.8 Å toward $C_f$ and a motion of 0.3 Å of the ester toward the approaching $OH^-$. The bond lengths within the resulting adduct are presented in Table 2. Application of the MBSE corrections to the points J, K, and L yields the energy profile shown in Fig. 4.

After the proton transfer has been completed, the imidazolium cation is free to rotate to its most stable position (M in Fig. 3). Here it forms a strong hydrogen bond to $O_s$ as well as weaker ones to formate (see Table 3). As shown by the branching in Fig. 4 there are now two possibilities. The first alternative is for the imidazolium to continue rotating up towards formate (N) and transfer a proton to $O_{a2}$ to form neutral imidazole and formic acid (O). Imidazole then rotates back down to (P) approximately the same position as in M. This branch will lead to a net stabilization of the system of 4 kcal and to an intermediate. The breakdown of this intermediate occurs through a reversal of the steps M → P, i.e., imidazole must first be protonated by formic acid to yield the configuration M once again. A proton is then transferred to the leaving group methoxide, accompanied by a

§ See Fig. 2 of ref. 2. Also, see the description of the reaction of formamide with two water molecules below.

¶ As mentioned above, this optimization does not include any change in $r(C_f—H_f)$ or in the coordinates of the $CH_3O$ group (except for a $C_f—O_s$ stretch). $r(O_w—H_{w2})$ is also held fixed.

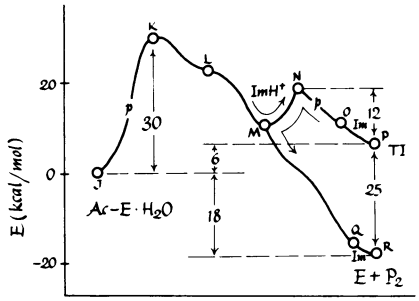


FIG. 4. Energy profile of deacylation of the model enzyme. Ac-E·$H_2O$ refers to configuration J in which a water molecule is noncovalently bound to the acyl enzyme. $P_2$ is HCOOH in our model system.

breakdown of the adduct. As the proton was transferred to $O_s$, the coordinates of methanol were optimized with respect to a retreat back to its original position in A. This was effected by a rotation about its $C_s$—$H_{s1}$ axis and a translation. As the hydrolyzed substrate HCOOH was pulled away from $O_s$, its internal coordinates were fully optimized except that $r(C_f$—$H_f)$ and $r(O_w$—$H_{w2})$ were held constant. In conformation Q, the hydrolyzed substrate has been removed and methanol is at its original position in the bound enzyme substrate complex E·S. Finally, an optimization of the imidazole position results in a configuration (R) identical to A except for the absence of the substrate. The TS for the breakdown of the TI (N) is encountered as a proton is transferred from formic acid to imidazole and the activation energy is 12 kcal/mol. The breakdown of the intermediate is exothermic by 25 kcal/mol.

As described above, following formation of the adduct (L), the imidazolium begins to rotate up away from $O_w$. Instead of rotating all the way up to formate, however, it may stop at its most stable position (M). A proton transfer to methoxide then results in the breakdown of the adduct and removal of the hydrolyzed substrate just as before (M–R). In bypassing segment M–P, this branch will result in the absence of an observed intermediate in deacylation. Regardless of which path is followed, the process of deacylation is calculated to be exothermic by 18 kcal/mol.

It might be noted that the breakdown of the adduct in deacylation (M–Q) involves no energy barrier, largely because of the strong hydrogen bond between $N^{\epsilon 2}$ of imidazolium and $O_s$ in configuration M. A displacement of the proton of only 0.7 Å is necessary in order for it to transfer completely from $N^{\epsilon 2}$ to $O_s$. In contrast, the breakdown of the adduct in acylation (F–H) involves an energy barrier. The hydrogen bond between the imidazolium and the leaving group in configuration F is significantly weaker than the bond above (See Table 3), and the proton transfer to the leaving group requires a larger displacement of 1.1 Å, thus yielding the transition state G.

The interaction of formamide with two water molecules was studied. Starting from the microwave geometry of formamide the CO and CN bond lengths were optimized (the geometry used is given in ref. 7). The oxygen atom of the first water molecule ($O_1H_aH_b$) was placed along the central axis of formamide such that $\measuredangle C$–$O_1$–$H_{a,b}$ = 109.5°. $r(C$–$O_1)$ was optimized to 2.57 Å. The oxygen atom of a second water molecule ($O_2H_cH_d$) was positioned along the $O_1$–$H_a$ bond axis such that $<O_1$–$O_2$–$H_{c,d}$ = 109.5°. $r(O_1$–$O_2)$ was then optimized to 2.58 Å. The internal geometry of both water molecules was assumed to be tetrahedral. As $H_a$ is moved towards $O_2$ the corrected energy of the system increases (by 66 kcal/mol for full transfer by 0.64 Å), but at 83% transfer, where the corrected energy has increased by 50 kcal/mol, the interaction between $O_1$ and formamide becomes attractive. At this point, a translation of formamide towards $O_1$ by 0.2 Å and a bending of its three substituents about C and away from $O_1$ result in a calculated (PRDDO) stabilization of the system. Further proton transfer and corresponding decrease of $r(C$–$O_1)$ lead to additional stabilization and eventually to the production of the tetrahedral adduct $HCO(NH_2)OH^-$, similar to the reactions studied in ref. 7.

In both the acylation and deacylation steps of our model enzyme the nucleophile delayed its attack upon the carbonyl group until it had acquired substantial negative charge. In our model enzyme, and presumably in the enzyme itself, most of the motion in nucleophilic attack is made by the nucleophile. The behavior of the above system in which the carbonyl group performs the required motion indicates that our results are not an artifact of the way in which our model enzyme was constructed. The development of considerable negative charge on the nucleophile in order for attack to take place appears instead to be a more general requirement.

## DISCUSSION

The catalytic mechanism of this model system is in accord with experimental results. Acylating agents (8, 9) indicate some freedom of His-57, and the rotation of Ser-195 as it attacks substrate is 20° in the x-ray study (5) and 30° in our study here. Proton transfer, as part of the rate-determining step in both acylation and deacylation, is consistent with deuterium isotope effects (1). For the acylation of the amide substrate, our result that the rate is determined by breakdown of the TI is in agreement with experiment (10). For esters, complications arise, depending on how good a leaving group occurs in the substrate. Our theoretical result, that esters behave like amides, assumes essentially the same geometry for these classes of substrates. However, esters are normally much less rigid than peptides, and hence we modify the picture for esters in the following way. After the TI has been formed, and the imidazolium has begun to approach the putative leaving group, we rotate the adduct $CH_3O$-$CHO(OH)^-$ 20° about its central C atom. The O atom of the leaving group ($O_e$) is then close enough to $N^{\epsilon 2}$ of imidazole to form a strong hydrogen bond ($O_e$···$N^{\epsilon 2}$). Now, the imidazolium need not rotate quite so far from formate in order to protonate the leaving group. These changes stabilize the point F′ (Fig. 2) by some 20 kcal/mol, and the 2.6 Å distance from $O_e$ to $N^{\epsilon 2}$ facilitates the subsequent proton transfer and accompanying breakdown, without a barrier, of the adduct. Thus, the activation energy for breakdown of the TI is smaller than that for its formation. Our model also predicts that the formation of the TI is rate determining during deacylation, in accord with experiment (1).

In our model system, only a small fraction of the actual enzyme–substrate is present, so that many quantum mechanical, electrostatic, and other effects are not included explicitly. For example, the carbonyl oxygen of the scissile linkage is hydrogen bonded to two residues in the enzyme (8). As this oxygen acquires a formal negative charge in the adduct, these hydrogen bonds would strengthen. In a model in which one water molecule was hydrogen bonded to this oxygen atom this stabilization was 25 kcal/mol greater for the tetrahedral adduct (C) than for the formamide substrate (A). This additional interaction would uniformly stabilize segments C–F (Fig. 2) and L–P (Fig. 4) by about 25 kcal/

mol in our reaction profiles. Point G and the shoulder between M and Q would be lowered by perhaps half of this amount. An energy barrier may then develop between M and Q, but the remaining parts of these profiles would remain essentially unchanged. In the acylation step, both formation and breakdown of the TI become nearly thermoneutral. Breakdown remains rate determining for the amide substrate. However, for the adduct involving the model ester substrate the freedom allowed above makes formation of the TI rate determining. Points P and R now have nearly equal energies. However, if the free energy of loss of hydrolyzed substrate from the pocket is dominated by the energetics, the $E + P_2$ part of Fig. 4 would be destabilized and a reversal may occur between the energies of P and R. This reversal and the energy barrier which may exist between M and Q might result in observation of an intermediate in deacylation.

Also charge–dipole and dipole–dipole (permanent or induced) interactions occur between excluded atoms and atoms of the model. These interactions, not included here, may introduce strain but may stabilize charged states. An example may be the possible stabilization by the protein of the incipient $OH^-$ produced in the TS in the formation of the intermediate in the deacylation step. Although we have used the x-ray coordinates to simulate conformational changes of the important residues of the enzyme during the course of catalysis, some motions not anticipated here may be important. For example, some possible translational freedom of Asp-102 may stabilize states in which His-57 is positively charged. For these reasons, we feel that our detailed mechanism is qualitatively correct, but that the activation energies (which are probably upper limits) may be too large by a factor of 2 or 3 as compared with those observed experimentally (11).

The effect of general acid-base catalysis is qualitatively illustrated by the theoretical activation energy of 50 kcal/mol found for the uncatalyzed formation of a tetrahedral adduct from formamide and water. This value is greater by 16 kcal/mol than that for our model (Fig. 2), and probably illustrates the greater effectiveness of His-Asp over $H_2O$ as catalyst for nucleophilic addition. If only one third of this difference is effective the charge relay system enhances the rate over that for water by about $10^4$. The His-Asp dyad is also an effective proton donor, since the catalytic activity of chymotrypsin is greatly reduced when $N^{\epsilon 2}$ (His-57) is methylated (12).[‖]

[‖] Mock (13) has given unusual weight to a requirement that the proton donor and nucleophile function on opposite sides of the plane of a scissile peptide bond in a particular orientation related to initial distortion of that bond. Chymotrypsin violates these requirements.

In summary, the serine which attacks and adds to the substrate's carbonyl group becomes a powerful nucleophile as it transfers a proton to the basic His-Asp dyad. We find (2) that the buried Asp is the stronger base of this dyad, and that it is the ultimate proton acceptor of the charge relay (3). The substrate, His-57, and the rest of the enzyme are responsible for maintaining Asp-102 away from solvent in the hydrophobic environment, and His-57 acts as a proton relay between Asp-102 and other parts of the active site. The motility of His-57 is a vital part of the enzymic mechanism. In addition, Asp-102 may increase the proton affinity of His-57, as suggested in our model by a ~34% increase in proton affinity of this imidazole when formate anion is added to our otherwise intact model.

Thus we have outlined an energetically plausible catalytic mechanism for the serine proteinases. We have started from an enzyme–substrate model which neglects some aspects of strain which arise partly from binding of a longer substrate and partly from entropy of desolvation, and we have neglected other entropy effects as well.

We are grateful to R. Huber for the starting coordinates, to D. A. Kleier for many helpful discussions, to the National Institutes of Health Grant GM 06920 for support, and to the National Science Foundation for a predoctoral fellowship to S.S. The figures were drawn by Jean Evans.

1. Bender, M. L. & Kilheffer, J. V. (1973) *CRC Crit. Rev. Biochem.* **1**, 149–199; and references therein.
2. Scheiner, S., Kleier, D. A. & Lipscomb, W. N. (1975) *Proc. Nat. Acad. Sci. USA* **72**, 2606–2610.
3. Blow, D. M., Birktoft, J. J. & Hartley, B. S. (1969) *Nature* **221**, 337–340.
4. Halgren, T. A. & Lipscomb, W. N. (1973) *J. Chem. Phys.* **58**, 1569–1591.
5. Bode, W., Schwager, P. & Huber, R. (1975) in *Proceedings at the 10th Meeting Federation of European Biochemical Societies, Paris, 1975*, ed Raoul, Y. (ASP Biological and Medical Press, Amsterdam), pp. 3–20.
6. Ditchfield, R., Hehre, W. J. & Pople, J. A. (1971) *J. Chem. Phys.* **54**, 724–728.
7. Scheiner, S., Kleier, D. A. & Lipscomb, W. N. (1975) *J. Am. Chem. Soc.*, in press.
8. Rühlmann, A., Kukla, D., Schwager, P., Bartels, K. & Huber, R. (1973) *J. Mol. Biol.* **77**, 417–436.
9. Krieger, M., Kay, L. M. & Stroud, R. M. (1974) *J. Mol. Biol.* **83**, 209–230.
10. Caplow, M. (1969) *J. Am. Chem. Soc.* **91**, 3639–3645.
11. Rajender, S., Han, M. & Lumry, R. (1970) *J. Am. Chem. Soc.* **95**, 4050–4052.
12. Henderson, R. (1971) *Biochem. J.* **124**, 13–18.
13. Mock, W. L. (1975) *Bioorg. Chem.* **4**, 270–278.